DOI 10.1002/prca.200700522 *Proteomics Clin. Appl.* 2007, *1,* 1446–1461

RESEARCH ARTICLE

Oligodendrocytes secrete exosomes containing major myelin and stress-protective proteins: Trophic support for axons?

Eva-Maria Krämer-Albers[1], Niko Bretz[1], Stefan Tenzer[2]*, Christine Winterstein[1]*, Wiebke Möbius[3], Hendrik Berger[2], Klaus-Armin Nave[3], Hansjörg Schild[2] and Jacqueline Trotter[1]*

[1] Department of Biology, Unit of Molecular Cell Biology, University of Mainz, Germany
[2] Institute for Immunology, University of Mainz, Germany
[3] Department of Neurogenetics, Max Planck Institute of Experimental Medicine, Goettingen, Germany

Oligodendrocytes synthesize the CNS myelin sheath by enwrapping axonal segments with elongations of their plasma membrane. Spatial and temporal control of membrane traffic is a prerequisite for proper myelin formation. The major myelin proteolipid protein (PLP) accumulates in late endosomal storage compartments and multivesicular bodies (MVBs). Fusion of MVBs with the plasma membrane results in the release of the intralumenal vesicles, termed exosomes, into the extracellular space. Here, we show that cultured oligodendrocytes secrete exosomes carrying major amounts of PLP and 2′3′-cyclic-nucleotide-phosphodiesterase (CNP). These exosomes migrated at the characteristic density of 1.10−1.14 g/mL in sucrose density gradients. Treatment of primary oligodendrocytes with the calcium-ionophore ionomycin markedly increased the release of PLP-containing exosomes, indicating that oligodendroglial exosome secretion is regulated by cytosolic calcium levels. A proteomic analysis of the exosomal fraction isolated by sucrose density centrifugation revealed in addition to PLP and CNP, myelin basic protein (MBP) and myelin oligodendrocyte glycoprotein (MOG) as constituents of oligodendroglial exosomes, together with a striking group of proteins with proposed functions in the relief of cell stress. Oligodendroglial exosome secretion may contribute to balanced production of myelin proteins and lipids, but in addition exosomes may embody a signaling moiety involved in glia-mediated trophic support to axons.

Received: June 1, 2007
Revised: July 14, 2007
Accepted: August 1, 2007

Keywords:
Exosomes / Multivesicular body / Myelin / Oligodendrocytes / Proteolipid protein

Correspondence: Dr. Eva-Maria Krämer-Albers, Department of Biology/Unit of Molecular Cell Biology, Johannes Gutenberg University Mainz, Bentzelweg 3, 55128 Mainz, Germany
E-mail: emkraemer@uni-mainz.de
Fax: +49-6131-3923840

Abbreviations: CNP, 2′3′-cyclic-nucleotide 3′-phosphodiesterase; **ESCRT,** endosomal sorting complexes required for transport; **HS,** horse serum; **ILV,** intralumenal vesicle; **MAG,** myelin-associated glycoprotein; **MBP,** myelin basic protein; **MOG,** myelin oligodendrocyte glycoprotein; **MVB,** multivesicular body; **PLP,** proteolipid protein

1 Introduction

Oligodendrocytes are responsible for synthesis and maintenance of the myelin sheath in the CNS, mediating electric insulation and trophic support to axons [1–3]. During brain development, these cells produce large amounts of myelin membrane, which is wrapped and compacted around axons. Myelin has a unique biochemical composition reflected in a high content of sphingolipids and cho-

* These three authors contributed equally.

lesterol and the inclusion of myelin-specific proteins. Proteolipid protein (PLP) and myelin basic protein (MBP) are the two most abundant myelin proteins and together constitute 80–90% of the total myelin proteins. Several recent studies have addressed the total myelin proteome and report improved characterization of minor myelin proteins [4–7].

Myelin formation requires bidirectional axon-glia communication, sorting of myelin components, and directed membrane traffic [8–10]. Interestingly, trafficking of the major myelin protein PLP involves accumulation in late endosomal compartments of multivesicular and multilamellar appearance. Stimulation of oligodendrocytes with a secreted neuronal factor of unknown identity results in redistribution of PLP from late endosomes to the plasma membrane [11]. However, late endosomal multivesicular bodies (MVBs) can adopt several distinct fates [12]. In addition to backfusion of the intralumenal vesicles (ILVs) with the limiting membrane, MVB can be subjected to the lysosomal degradative pathway, or they can fuse with the plasma membrane releasing the ILV into the extracellular space, which then are termed exosomes. Remarkably, these exosomes display a membrane topology identical to the plasma membrane.

Release of membrane particles in the form of exosomes or exosome-like vesicles has been demonstrated for a large number of cell types. Although exosomes have mostly been isolated from the supernatants of cultured cells, their existence *in vivo* is not disputed, as exosomes can be isolated in large amounts from body fluids such as blood plasma and urine [13–16]. Exosomes are characterized by their small size of 50–100 nm and their specific cargo. Protein and lipid sorting occurs at the level of the limiting membrane of the MVB [17], where mono- and oligo-ubiquitinated proteins are recognized by a series of multiprotein complexes of the ESCRT (endosomal sorting complexes required for transport) machinery [18]. However, ESCRT and ubiquitin independent sorting to ILV or exosomes is also possible and generally involves association with membrane microdomains with characteristics of lipid rafts or tetraspanin-enriched microdomains [19, 20]. The cytoplasmic cargo of exosomes includes the ESCRT components Alix and Tsg101 as well as chaperones of the heat-shock protein family, cytoskeletal proteins, and enzymes.

The physiological role of exosomes is not fully understood [21]. Originally, exosomes were described as a mechanism for the removal of unneeded membrane during maturation of reticulocytes [22]. More recent work with immune cells has demonstrated that exosomes contribute to intercellular communication allowing transfer of molecules from one cell to another. The presence of MHC class I and class II antigens, as well as costimulatory and adhesion molecules, confers on exosomes the ability to modulate the immune response; however, both mediation of priming and tolerance induction are possible [23]. The transcellular signaling function of extracellular membrane particles is not limited to the immune system: studies performed with *Drosophila* and *C. elegans* suggest that exosome-like vesicles mediate the release and spread of morphogens and thus participate in tissue-specific developmental processes [24, 25].

Here, we show that myelinating oligodendrocytes secrete membrane particles with the characteristics of exosomes in a Ca^{2+}-dependent manner. Proteomic analysis of a purified oligodendroglial exosome fraction demonstrates the presence of genuine myelin proteins as well as proteins typically localized to exosomes in other cell types. Exosome release by oligodendrocytes may play a role in the disposal of redundant myelin proteins, or may contribute to glia-axon signaling.

2 Materials and methods

2.1 Reagents and antibodies

General chemicals were purchased from Roth (Karlsruhe, Germany) and Sigma (Munich, Germany). Di-butyryl-cyclic AMP, poly-L-lysine, aprotinin, leupeptin, Triton X-100, and Na-deoxycholate were from Sigma. Culture media, B27 supplement and serum were from Invitrogen (Karlsruhe, Germany). Human recombinant PDGF (AA) and bFGF were from TEBU (Frankfurt, Germany). Ionomycin-Ca^{2+} was from Calbiochem. Bradford reagent for protein assays was from BioRad (München, Germany). PVDF-membrane was from Millipore (Bedford, USA). ECL Supersignal reagent was from Perbio (Bonn, Germany), ECL Hyperfilms and [1-^{14}C]sodium acetate were from GE-Healthcare (Freiburg, Germany).

The following antibodies were used: anti-PLP, clone AA3 (Dr. M. B. Lees, Waltham, MA) and polyclonal A431 (K. Nave, Göttingen, Germany), anti-myelin oligodendrocyte glycoprotein (MOG), clone 8-18-C5 (C. Linington, Aberdeen, Scotland), anti-myelin-associated glycoprotein (MAG), clone 513 (M. Schachner, Hamburg, Germany), anti-2′3′-cyclic-nucleotide 3′-phosphodiesterase (CNP) (Sigma), anti-Alix, clone 49 (BD Transduction Laboratories, Erembodegem, Belgium), anti-Tsg101, clone 4A10 (GeneTex, San Antonio, TX, USA), anti-calreticulin (Stressgen Biotechnologies, Victoria, BC, Canada), anti-Na^+/K^+-ATPase, clone 464.6 (Novus Biologicals, Littletan, CO, USA). All secondary antibodies were purchased from Dianova (Hamburg, Germany).

2.2 Cell culture

Primary cultures of oligodendrocytes were prepared from embryonic day 14–16 mice as described [26]. Briefly, oligodendrocytes growing on top of astrocyte monolayers were shaken off and plated in modified Sato medium [27] supplemented with B27 and 1% horse serum (HS) on poly-L-lysine

coated dishes (8×10^6 cells/60 mm dish). To promote survival of the cells, 10 ng/mL human recombinant platelet-derived growth factor (AA) and 5 ng/mL basic fibroblast growth factor were added immediately after plating. Oligodendrocytes were kept for 7 days *in vitro* without additional growth factors before harvesting cells and culture supernatant. The oligodendroglial precursor cell line Oli-neu was cultured in Sato, 1% HS and treated with 1 mM di-butyryl-cyclic AMP for 3 days to induce differentiation [28]. All cells were cultured at 37°C, 5% CO_2, and 95% humidity.

2.3 Cell lysates and exosome isolation

2.3.1 Cell lysates

Primary oligodendrocytes or Oli-neu cells (8×10^6 or 1×10^6, respectively) were scraped in 1 mL 10 mM Tris pH 7.4, 150 mM NaCl, 1 mM EDTA, 1% Triton X-100, 0.5% DOC, 1 μg/mL aprotinin, 5 μg/mL leupeptin, and 1 mM PMSF on ice. Nuclei were pelleted by centrifugation for 10 min at $300 \times g$. The protein concentration of nuclei-free lysates was determined by Bradford assay and 5–10 μg of total protein was loaded on SDS-PAGE gels.

2.3.2 Exosome isolation

The culture supernatant of primary oligodendrocytes (4–6×10^7 cells) was collected either over 7 days, or at day 7 the cells were washed two times with 150 mM NaCl, 8 mM Na_2HPO_4, 1.7 mM NaH_2PO_4, pH 7.4 (PBS) and further cultured with serum-free medium for defined collection periods (ionomycin treatment and proteomics, see below). Oli-neu cells were grown to 70–80% confluency (1×10^7 cells), washed and cultured in serum-free Sato-medium for another 24 h. Culture supernatants of primary oligodendrocytes or Oli-neu cells were collected and cleared from debris by successive centrifugation for 10 min at $60 \times g$ and 20 min at $10\,000 \times g$ and 4°C. Small membrane particles remaining in the supernatant were pelleted by ultracentrifugation for 2 h at $100\,000 \times g$ and 4°C. For initial characterization, the pellet was resuspended in 80 μL SDS-PAGE sample buffer and subjected to SDS-PAGE and Western blotting (20 μL *per* lane). For further purification, the pellet was resuspended in 50 mM Tris pH 7.4, 150 mM NaCl (TBS) and layered on top of a gradient of 0.3–1.8 M sucrose in TBS. Following centrifugation at $100\,000 \times g$ for 16 h, 200 μL fractions were collected, their density was determined using a refractometer (Master-T and Master-2T, Atago, Tokyo, Japan) and 30 μL *per* fraction were analyzed by SDS-PAGE and Western blotting. To obtain exosome preparations clean from serum contaminants for proteomic analysis, primary oligodendrocytes (6×10^7 cells) differentiated for 7 days *in vitro* were washed two times with PBS and further cultured with serum-free Sato-medium. Exosome containing supernatants were obtained by three successive collection periods of 24 h duration and exosomes were isolated by density gradient centrifugation. Exosome containing gradient fractions were pooled, diluted to 0.5 M Sucrose with TBS, and ultracentrifuged for 1 h at $100\,000 \times g$ and 4°C to pellet exosomes.

2.3.3 Ionomycin treatment

To stimulate exosome release by increasing the free cytoplasmic Ca^{2+} levels, primary oligodendrocytes cultured for 7 days were treated with 1 μM ionomycin-Ca^{2+}. Cells were washed two times with PBS and incubated for up to 2 h in serum-free Sato/B27 medium containing 1 μM ionomycin. Control cells were incubated in medium without ionomycin. After the treatment period, the medium was collected and exosomes were isolated by differential centrifugation (2×10^7 cells *per* condition) or density gradient centrifugation (4×10^7 cells *per* condition) as described above.

2.4 Membrane preparation and myelin isolation

Total membranes were prepared as described [26]. Briefly, a postnuclear supernatant was prepared from primary cultured oligodendrocytes by scraping cells in 10 mM Tris, pH 7.4 and shearing cells through a 22 gauge needle followed by centrifugation for 10 min at $200 \times g$ and 4°C. Membranes were pelleted by ultracentrifugation for 30 min at $100\,000 \times g$. Myelin was prepared from the brains of adult NMRI mice of both sexes using discontinuous sucrose density gradient centrifugation [29]. Briefly, brains were homogenized in ice-cold 10.5% sucrose with the help of an Ultra-Turrax T25 (IKA, Staufen, Germany). Myelin was removed from the interface between 10.5 and 30% sucrose gradients and subjected to two rounds of hypo-osmotic shock by resuspension in a large volume of ice-cold water and reisolation on the discontinuous sucrose gradient (this separates myelin membranes from axolemma). Purified myelin was collected from the final sucrose interface, washed twice with cold water, and resuspended in a small volume of PBS.

2.5 SDS-PAGE and Western blotting

SDS-PAGE analysis of proteins was performed using self-made 8 or 10% gels as described [30] or 4–12% NuPAGE gels according to the manufacturer's instructions (Invitrogen). In general, gels were run under reducing conditions, unless otherwise noted. Proteins were transferred to a PVDF membrane by semidry blotting and the membrane was blocked with 4% milkpowder, 0.1% Tween in PBS. Proteins were detected by sequential incubation of the membrane with primary antibodies overnight at 4°C and second antispecies antibodies conjugated with HRP for 30–60 min at room temperature. The blots were developed by ECL according to the manufacturer's instructions. In some cases, membranes were stripped with 100 mM glycine pH 2 for 30 min, blocked, and reprobed with antibodies.

2.6 Electron microscopy

2.6.1 Immunoelectron microscopy

Primary oligodendrocytes were fixed in 4% formaldehyde and 0.2% glutaraldehyde in 0.1 M phosphate buffer. After washing, the cells were scraped from the dish in 0.1 M phosphate buffer containing 1% gelatine, spun down and resuspended in 10% gelatine in 0.1 M phosphate buffer at 37°C. After spinning down, the pellets in gelatine were cooled on ice, removed from the tubes and cut in small blocks. These blocks were infiltrated in 2.3 M sucrose in 0.1 M phosphate buffer, mounted onto aluminum pins for ultramicrotomy and frozen in liquid nitrogen. Ultrathin cryosections were picked up according to Liou *et al.* [31] in a 1:1 mixture of 2% methylcellulose and 2.3 M sucrose. For immuno-labeling, sections were incubated with A431 antibodies specific for PLP, which was detected with protein A-gold (10 nm). Sections were analyzed with a LEO EM912 Omega electron microscope (Zeiss, Oberkochen) and digital micrographs were obtained with an on-axis 2048 × 2048-CCD camera (Proscan, Scheuring).

2.6.2 Whole mount and negative staining

Exosomes and membranes from the 100 000 × *g* fraction were fixed by the addition of formaldehyde resulting in a final concentration of 4%. The fraction was adsorbed to a formvar-carbon-coated grid by floating the grid for 10 min on 5 μL droplets on parafilm. For negative staining, the grid was rinsed in water and floated for 5 min on a droplet of 2% neutral uranyl acetate, containing 0.7 M oxalate, titrated with ammonium hydroxide to a pH of 7. Then the staining solution was removed by holding the grid with forceps on a piece of filter paper. After air-drying the grid was examined with the electron microscope. In case of whole mount electron microscopy, the grids were rinsed in PBS and water and floated for 5 min on 2% neutral uranyl acetate, containing 0.7 M oxalate, titrated with ammonium hydroxide to a pH of 7. After embedding the adhering vesicles and membranes in a mixture of 1.8% methylcellulose and 0.4% uranyl acetate [31] the grid was examined with the electron microscope.

2.7 Identification of proteins by MS

2.7.1 Protein digest preparation

Pelleted exosomes from three different preparations (described under Section 2.3) were pooled and subjected to proteomic analysis. Exosomes were solubilized in 25 mM ammonium bicarbonate containing 0.1% RapiGest (Waters, Eschborn, Germany; 80°C, 15 min). Proteins were reduced by adding 5 mM DTT (45 min, 56°C) and free cysteines alkylated with iodoacetamide (Sigma, Taufkirchen, Germany; 15 mM, 25°C, 1 h in dark). Porcine (0.2 μg) sequencing grade trypsin (Promega, Mannheim, Germany) were added and the samples were incubated overnight at 37°C. After digestion, RapiGest was hydrolyzed by adding 10 mM HCl (37°C, 10 min) and the resulting precipitate was removed by centrifugation (13 000 × *g*, 15 min, 4°C) and the supernatant was transferred into an autosampler vial for peptide analysis *via* LC-MS.

2.7.2 UPLC configuration

Capillary LC of tryptic peptides was performed with a Waters NanoAcquity UPLC system equipped with a 75 μm × 150 mm BEH C18 RPRP column and a 2.6 μL PEEKSIL-sample loop (SGE, Darmstadt, Germany). The aqueous mobile phase (mobile phase A) was H_2O (LC-MS Grade, Roth, Freiburg, Germany) with 0.1% formic acid. The organic mobile phase (mobile phase B) was 0.1% formic acid in ACN (LC-MS grade, Roth). Samples (2.6 μL injection) were loaded onto the column in direct injection mode with 3% mobile phase B for 15 min at 400 nL/min, followed by an additional 10 min wash (3% B) for 10 min at 300 nL/min. Peptides were eluted from the column with a gradient from 3−35% mobile phase B over 90 min at 300 nL/min followed by a 20 min rinse of 80% mobile phase B. The column was immediately re-equilibrated at initial conditions (3% mobile phase B) for 20 min. [Glu^1]fibrinopeptide was used as lockmass at 300 fmol/μL. Lockmass solution was delivered from the auxiliary pump of the NanoAcquity system at 400 nL/min to the reference sprayer of the NanoLockSpray™ source. Samples were analyzed in triplicate.

2.7.3 Mass spectrometer configuration

MS analysis of tryptic peptides was performed using a Waters Q-TOF Premier API system, operated in V-mode with typical resolving power of at least 10 000. All analyses were performed using positive mode ESI using a NanoLockSpray source. The lock mass channel was sampled every 30 s. The mass spectrometer was calibrated with a [Glu^1]fibrinopeptide solution (300 fmol/μL) delivered through the reference sprayer of the NanoLockSpray source. Accurate mass LC-MS data were collected in an alternating, low energy (MS) and elevated energy (MS^E) mode of acquisition. The spectral acquisition time in each mode was 1 s with a 0.05-s interscan delay. In low energy MS mode, data were collected at a constant collision energy of 3 eV. In MS^E mode, collision energy was ramped from 16 to 32 eV during each 1-s data collection cycle. One cycle of MS and MS^E data was acquired every 2.1 s. The radio frequency applied to the quadrupole mass analyzer was adjusted such that ions from m/z 300 to 1500 were efficiently transmitted, ensuring that any ions observed in the LC-MS^E data less than m/z 300 were known to arise from dissociations in the collision cell.

2.7.4 Data processing and protein identification

The continuum LC-MS^E data were processed and searched using the IDENTITY^E- Algorithm of ProteinLynx Global Server (PLGS) version 2.3. The resulting peptide and protein identifications were evaluated by the software using statistical models similar to those described by Skilling *et al.* [32]. Protein identifications were assigned by searching the UniProtKB/Swiss-Prot Protein Knowledgebase Release 52.3 for mouse proteins (12 920 entries) supplemented with known possible contaminants (porcine trypsin, human keratins) using the precursor and fragmentation data afforded by the LC-MS acquisition method as described before [33–35]. The search parameter values for each precursor and associated fragment ions were set by the software using the measured mass error obtained from processing the raw continuum data. Peptide identifications were restricted to tryptic peptides with no more than one missed cleavage. Carbamidomethyl cysteine was set as fixed modification, and oxidized methionine, protein N-acetylation, and deamidation of asparagine and glutamine were searched as variable modifications. Database search was performed allowing a maximal mass deviation of 15 ppm for precursor ions and 30 ppm for fragment ions. For a valid protein identification, the following criteria had to be met: at least two peptides detected with together at least seven fragments. All reported peptide identifications provided by the IDENTITY^E-algorithm are correct with >95% probability [36]. The false positive rate for protein identification was set to 1% based on search of a reversed database, which was generated automatically using PLGS 2.3 by reversing the sequence of each entry. By using replication as a filter, the false positive rate is further minimized, as false positive identifications do not tend to replicate across injections due to their random nature [35].

2.7.5 Annotation of protein function and prediction of subcellular localization of identified proteins

Prediction of subcellular localization was performed using the WoLF Psort protein localization predictor [37] or ProteinCenter (www.proxeon.com). Annotation of protein function was performed using the Open Access version of Protein Center.

2.8 Lipid analysis

Primary oligodendrocytes (2×10^7 cells) cultured for 4 days were washed and labeled for 48 h at 37°C with 20 μCi/mL [1-^{14}C]sodium acetate in serum-free Sato/B27 medium to achieve radiolabeling of lipids. Culture supernatants were collected and subjected to exosome purification utilizing density gradient centrifugation. Exosome containing gradient fractions were pooled, diluted with TBS, and ultracentrifuged for 1 h at 100 000 × *g* and 4°C to pellet exosomes. Total membranes were isolated from the remaining cells as described above. Lipids were extracted from pelleted exosomes, total oligodendroglial membranes, and isolated myelin as described [38]. Dried samples were dissolved in 10–20 μL of chloroform/methanol (1:1 v/v) and spotted on activated Silica Gel 60 F_{254} plates (Merck, Darmstadt, Germany). After resolution of the lipids in chloroform/methanol/H_2O (65:25:4 v/v) the plates were air-dried and reference lipids and myelin lipids were visualized by exposure of the plates to 10% sulfuric acid, 5% methanol, and charring for 20 min at 140°C. Radiolabeled lipids were detected by autoradiography.

3 Results

3.1 Oligodendrocytes secrete exosomes containing PLP

In primary cultured oligodendrocytes, in the absence of neurons, a large proportion of PLP is found in LAMP1-positive late endosomal compartments [8, 11, 39]. To resolve the ultrastructure of PLP-containing intracellular organelles we performed immunoelectron microscopy. PLP-containing endosomes of both multilamellar and MVB were observed (Fig. 1). In MVB, PLP localized to the limiting membrane and was also present in the membrane of the ILV. We thus tested if exosomes are found in the culture supernatant of primary cultured oligodendrocytes and of the oligodendroglial cell line Oli-neu [28]. Culture supernatants were subjected to differential centrifugation and pelleted membrane particles were analyzed by Western blotting using antibodies directed against the myelin proteins PLP, MAG, MOG, and CNP. As a positive identification for exosomes we used antibodies specific for Alix, a previously described cytoplasmic cargo protein of exosomes [40, 41], while Na^+/K^+-ATPase antibodies served as a control for contaminating plasma membrane. The 100 000 × *g* pellets of culture supernatants collected from primary oligodendrocytes contained PLP, CNP, and Alix, but were negative for the myelin proteins MAG and MOG (Fig. 2A). PLP occurs in two isoforms of 26 or 20 kDa (PLP and DM20, respectively) and can form oligomers. The two isoforms of PLP were equally represented in the membrane pellets of the culture supernatant; however, PLP dimers were more strongly represented in the pellet in relation to the total cell lysate. Marker proteins of the plasma membrane (Na^+/K^+-ATPase, Fig. 2A), ER (calreticulin, not shown), and Golgi membranes (GM130, not shown) were not detected in the 100 000 × *g* pellets from supernatants. Oli-neu cells treated with di-butyryl-cyclic adenosine monophosphate to induce differentiation and concomitant expression of endogenous PLP also secreted membrane-associated PLP into the culture supernatant (Fig. 2B; MAG, MOG, and CNP were not detectable by Western blot in the total cell lysates and thus are not shown). To ensure that the results were not falsified by exosomal contaminants derived from the 1% HS supplemented in the medium, we tested 100 000 × *g* pellets of medium containing 10% HS and did

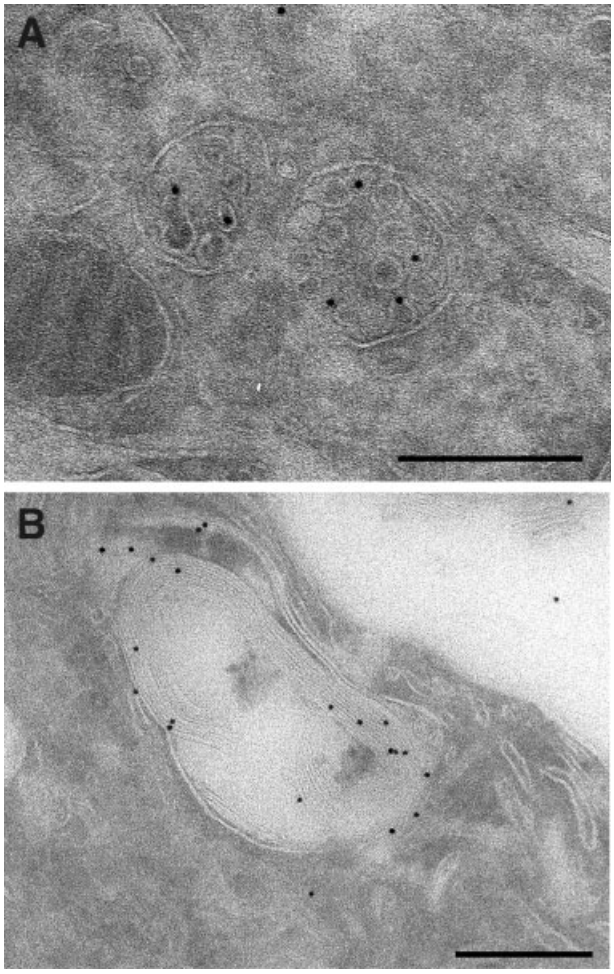

Figure 1. Electron micrographs of immunolabeled primary cultured oligodendrocytes using antibodies recognising PLP. PLP is associated with the ILVs of MVBs (A) and multilamellar bodies (B) located in the cytoplasm of primary oligodendrocytes. Bars, 250 nm.

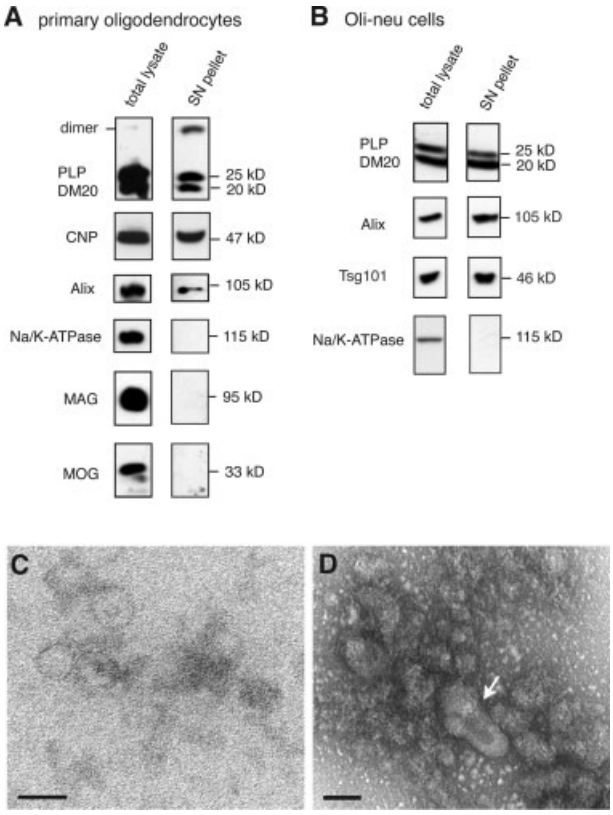

Figure 2. Oligodendroglial cells secrete vesicular membrane particles containing PLP and exosomal marker proteins. (A, B) Western blot analysis of total cell lysates and membrane vesicles pelleted by differential centrifugation from culture supernatants (SN pellet) of (A) primary cultured oligodendrocytes or (B) Oli-neu cells. In addition to the exosomal marker Alix, the myelin proteins PLP and CNP were associated with microvesicles secreted by the cells, while other myelin proteins such as MAG and MOG were not detected. Na^+/K^+-ATPase was used as a general control for plasma membrane fragments. (C) Whole mount transmission electron micrograph and (D) negative staining of exosome-like microvesicles, pelleted from the culture supernatants of primary oligodendrocytes. Occasionally, multilamellar structures (white arrow) are seen between unilamellar vesicles. Bars, 50 nm.

not find any exosomal components (not shown). We further elucidated the ultrastructure of the pelleted membrane particles by whole-mount electron microscopy. The main part of the isolated membranes were vesicles of spherical shape and had an average diameter of 30–80 nm (Fig. 2C), fitting the morphological criteria of exosomes. Ocassionally, multilamellar membrane structures were found in between the unilamellar microvesicles.

However, differential centrifugation of culture supernatants does not unambiguously discriminate between secreted exosomes and other type of vesicular membranes shed by the cells. To further elucidate the nature of the membrane particles released by oligodendroglial cells, we subjected the $100\,000 \times g$ pelleted membranes to sucrose density gradient centrifugation, where exosomes float at a density around 1.13 g/mL with variations depending on the cell type [13]. We determined the distribution of Alix and PLP within the gradient by Western blotting of the gradient fractions and found codistribution of the two proteins (Fig. 3). The peak fraction of both proteins exhibited a density of 1.116 g/mL. As expected, Na^+/K^+-ATPase was not detectable in any of the gradient fractions. Taken together, oligodendrocytes secrete vesicular membrane particles with the typical characteristics of exosomes.

3.2 Oligodendroglial exosome release is stimulated by elevated intracellular Ca^{2+} levels

Fusion of late endosomal MVB with the plasma membrane may occur in analogy to the secretion of lysosome-related organelles, which is regulated by Ca^{2+} [42, 43]. We next tested

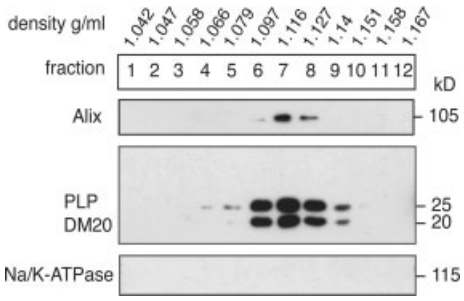

Figure 3. Purification of exosomes from primary cultured oligodendrocytes by density gradient centrifugation. Exosome-like membranes pelleted from culture supernatants were separated on a continuous sucrose density gradient and fractions anaylzed by Western blotting. PLP comigrates with the exosomal marker Alix in gradient fractions of density 1.097–1.127 g/mL. The PLP signal was confined to monomeric PLP and DM20 and thus the region of the gel where PLP dimers run is not shown. The absence of a signal for the Na^+/K^+-ATPase demonstrates that plasma membrane derived membranes were not present in the gradient.

whether exosome release by oligodendroglial cells is Ca^{2+}-dependent. We made use of the ionophore ionomycin, which allows entrance of Ca^{2+} ions into the cytoplasm and thus results in elevation of the free cytoplasmic Ca^{2+}-levels. Primary cultured oligodendrocytes were washed and incubated in serum-free medium with or without 1 μM ionomycin. As shown in Fig. 4A, the cellular integrity was not affected by the ionomycin treatment, and we did not observe any signs of membrane detachment or apoptosis. After different treatment times, the culture supernatant was collected, subjected to differential centrifugation, and the level of membrane-associated PLP in the pellet was determined. Ionomycin treatment of oligodendrocytes over 30, 60, and 120 min was accompanied by a steady increase in the level of membrane-associated PLP isolated from the culture supernatant and after 120 min the release was strongly enhanced compared to the basal level of release of untreated cells (Fig. 4B). Fractionation of the pelleted membranes by sucrose density gradient centrifugation confirmed the increased release of

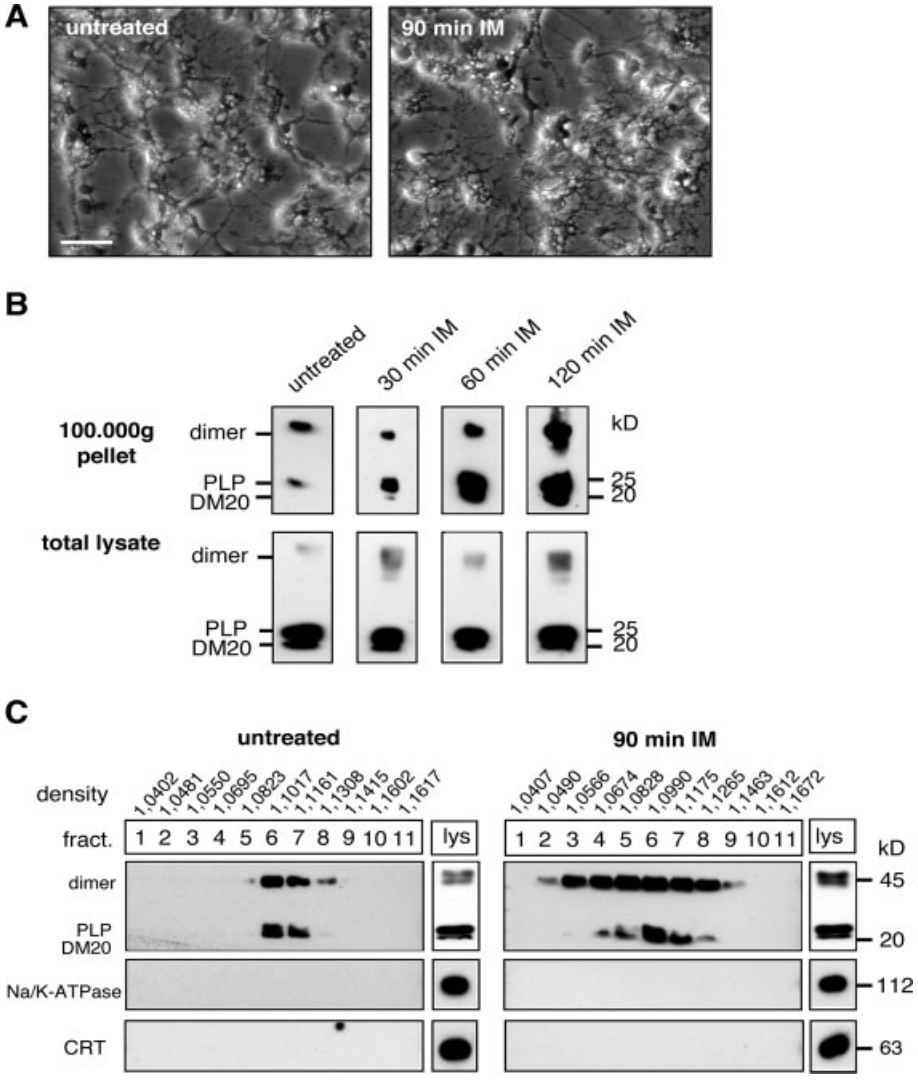

Figure 4. The release of PLP-containing exosomes is stimulated by the Ca^{2+}-ionophore ionomycin. (A) Phase contrast picture of primary oligodendrocytes treated for 90 min with 1 μM ionomycin. Treated cells appear viable and do not lift or retract their processes. (B) Exosomes pelleted by differential centrifugation from culture supernatants collected from cells treated for 30, 60, or 120 min with 1 μM ionomycin or left untreated for 120 min were analyzed by Western blotting using antibodies against PLP (upper panels). Normalized to the total cell lysates (lower panel), the secretion of membrane-associated PLP into the culture supernatant increases over 120 min of ionomycin treatment. (C) Exosomes collected from supernatants of cells treated with ionomycin or left untreated over 90 min were fractionated by sucrose density gradients and analyzed by Western blotting with antibodies against PLP, Na^+/K^+-ATPase, and calreticulin. Note that the gel was run under non-reducing conditions, thus favoring the preservation of dimeric PLP. IM, ionomycin; fract., fraction number; CRT, calreticulin.

PLP-containing membranes by ionomycin treated cells and showed peaks in the typical exosome fractions (Fig. 4C). However, in case of analysis under nonreducing conditions, the dimeric form of PLP seemed to be elevated compared to the monomer and was additionally present in fractions of lower density (under reducing conditions only the monomic PLP and DM20 were visible; not depicted). Possibly, exosomes released in response to ionomycin stimulation exhibit a greater heterogeneity. Multilamellar bodies may also be stimulated by ionomycin to fuse with the plasma membrane and release multilamellar membranes into the supernatant, which would be expected to exhibit lower density. Contamination of the gradient fractions by plasma membrane or ER membranes (released by stressed cells during ionomycin treatment) was ruled out by blotting the gradient fractions with antibodies against Na^+/K^+-ATPase and calreticulin. We were unable to detect Alix or Tsg101 in these experiments, neither in the $100\,000 \times g$ pellets nor in the gradient fractions, most likely because it was below detection levels after such short release times.

When ionomycin-treated oligodendrocytes were subjected to immunoelectronmicroscopy we occasionally observed fusion profiles of late endosomal organelles, some of which contained ILV carrying PLP (Fig. 5A, arrow and inset). Moreover, groups of exosome-like vesicles labeling with PLP antibodies, were localized outside the cells in the vicinity of the oligodendroglial plasma membrane (Fig. 5B, arrows).

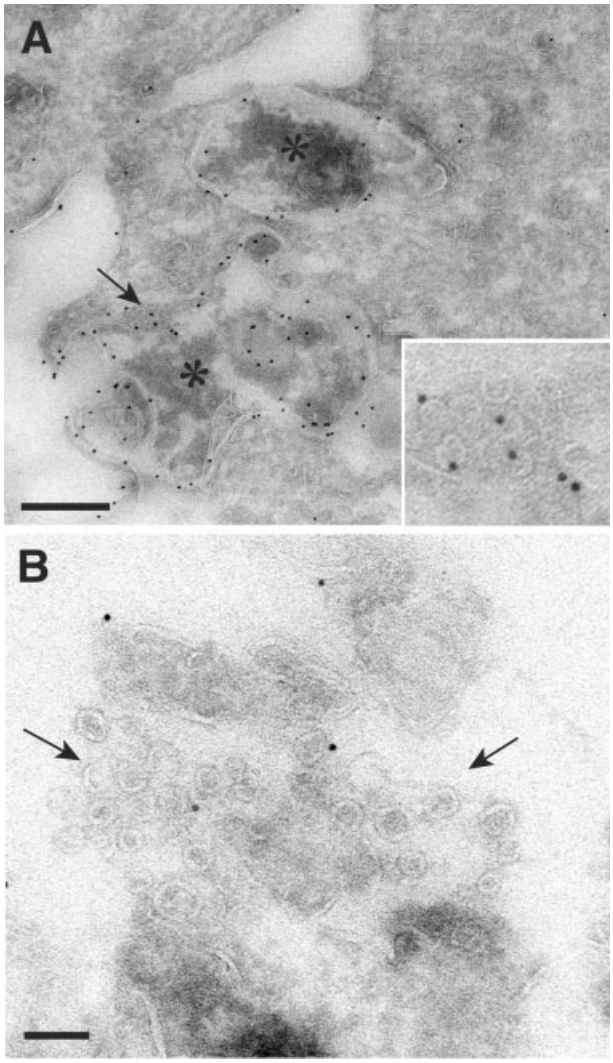

Figure 5. Immunoelectron microscopy of primary cells treated for 90 min with 1 μM ionomycin and immunolabeled with antibodies recognising PLP. (A) Fusion profiles of late endosomal vesicles with the plasma membrane (asterisk), some of which are filled with PLP-containing ILVs (arrow) are shown. The ILV marked by the arrow are enlarged in the inset. Bar, 400 nm. (B) Groups of exosome-like vesicles (arrows) labeling with PLP antibodies are observed at the extracellular surface of the cells. Bar, 100 nm.

3.3 Proteomic characterization of oligodendroglial exosomes

To shed light on the specific cargo of oligodendroglial exosomes we performed proteomic analysis of exosomes isolated from density gradient fractions. We pooled fractions 6–9 corresponding to a density of 1.10–1.14 g/mL and pelleted the membranes by ultracentrifugation. Pelleted exosomes were solubilized in 25 mM ammonium bicarbonate, 0.1% RapiGest, digested with trypsin, and analyzed by nanoUPLC-MS in LC-MS^E acquisition mode on a QTOF Premier mass spectrometer. Samples were analyzed in triplicates. In three runs, we identified a total of 143 proteins (Supporting Information, Table S1), of which 83 (58%) were detected in all runs and 23 (16%) were detected in two runs. The false positive rate for protein identification was set to 1% for a single run. By using replication as a filter, the false positive rate is further reduced [35] (Table 1). Predictions of subcellular localization (Fig. 6A, Supporting Information, Table S1) performed by WoLF Psort [37] and ProteinCenter software however generated divergent results, thus demonstrating that the algorithms of these programs imply distinct rules for prediction. The WoLF Psort algorithm assigned most proteins to the cytosol, while ProteinCenter affiliated the results preferentially to membrane and nucleus. When ProteinCenter software was applied to assign potential functions to the identified exosomal proteins, an emphasis towards functions in metabolism, biogenesis, cell organization and regulation became evident (Fig. 6B). A considerable number of proteins also classified to processes such as transport, cell communication, and development.

However, since the application of algorithms has its restrictions, we performed an independent classification according to information obtained from Swiss-Prot entries and the literature (Fig. 6C and Table 1). We then matched our results with exosomal proteins identified by previous studies in other cell types, namely dendritic cells [41], B-cells [44], microglia [45], mesothelioma [46], melanoma [47], cortical

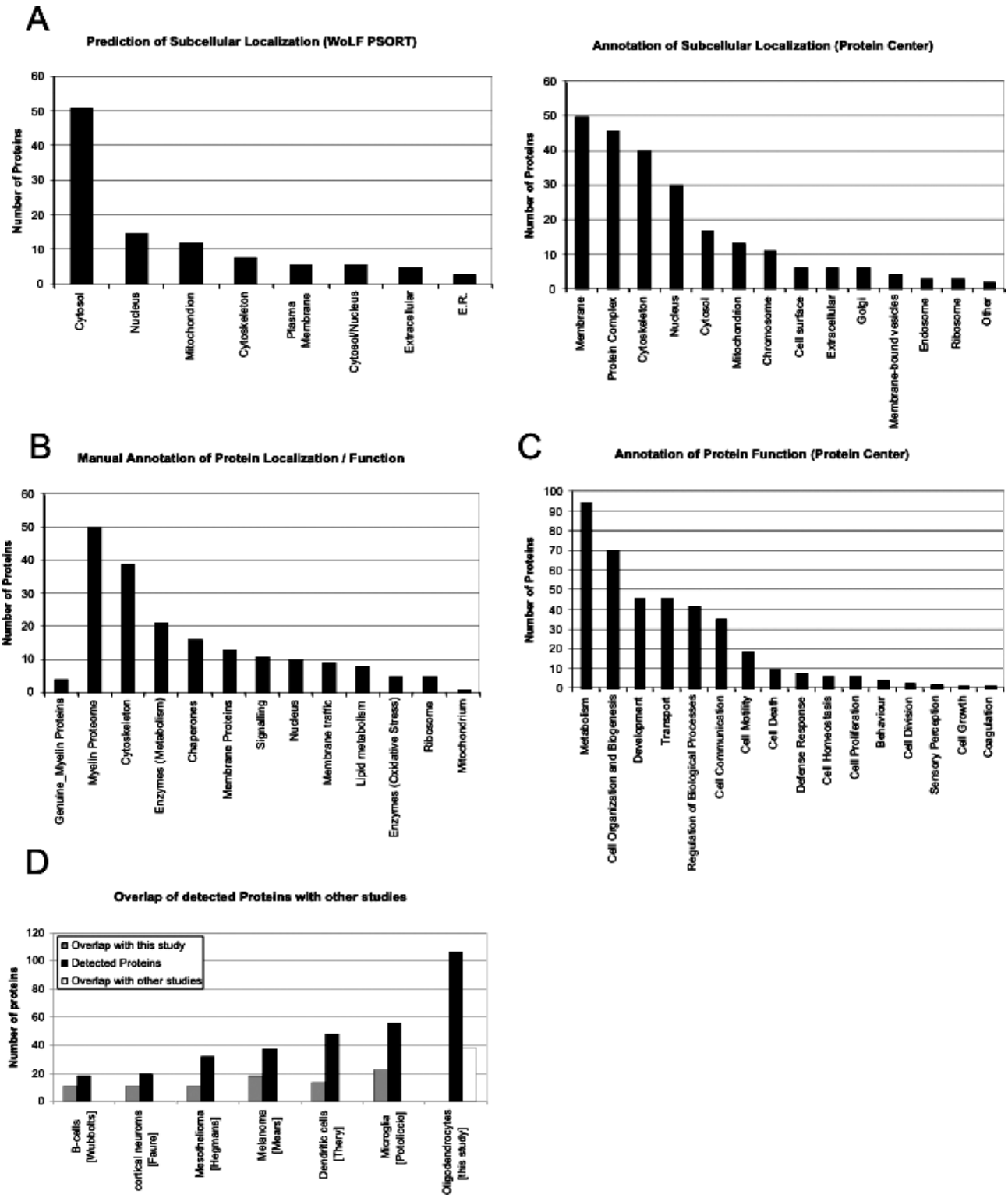

Figure 6. Proteomic analysis of proteins detected in oligodendrocyte-derived exosomes. (A) Subcellular localization predictions using WoLF-PSORT (left panel) or Protein Center Software (right panel). (B) Annotation of protein function using Protein Center Software. (C) Manual annotation of protein localization/function according to Swiss-Prot classification and published literature. (D) Overlap of proteins detected in this study with previously published data on exosomes from defined cell types. Black bars, total proteins detected; gray bars, overlap with this study; white bar, proteins previously described as exosomal proteins by other studies. Only proteins detected in at least two runs were taken into account.

Table 1. Proteins identified in purified oligodendroglial exosomes by LC-MS^E in at least two runs

	Detected	Accession	Entry	Description	Myelin proteome	References
Myelin proteins	3	P16330	CN37_MOUSE	CNP	X	[44]
(genuine)	3	P04370	MBP_MOUSE	MBP	X	
	2	Q61885	MOG_MOUSE	MOG	X	
	3	P60202	MYPR_MOUSE	Myelin PLP	X	
Membrane	3	Q8VDN2	AT1A1_MOUSE	Sodium potassium transporting ATPase alpha 1 chain	X	[42]
proteins	3	Q6PIE5	AT1A2_MOUSE	Sodium potassium transporting ATPase alpha 2 chain	X	
	2	Q6PIC6	AT1A3_MOUSE	Sodium potassium transporting ATPase alpha 3 chain		[43]
	2	Q9WV27	AT1A4_MOUSE	Sodium potassium transporting ATPase alpha 4 chain	X	
	3	P35762	CD81_MOUSE	CD81 antigen	X	[43]
	3	Q8R366	IGSF8_MOUSE	Ig superfamily member 8	X	[45]
Cytoskeleton	3	P62737	ACTA_MOUSE	Actin aortic smooth muscle alpha actin 2		
	3	P60710	ACTB_MOUSE	Actin cytoplasmic 1 beta actin	X	[43–45]
	2	P63260	ACTG_MOUSE	Actin cytoplasmic 2 gamma actin	X	[39, 42, 45, 46]
	3	P18760	COF1_MOUSE	Cofilin 1	X	[39, 43]
	3	P13020	GELS_MOUSE	Gelsolin	X	[46]
	3	P02535	K1C10_MOUSE	Keratin type I cytoskeletal 10	X	[45]
	3	P08730	K1C13_MOUSE	Keratin type I cytoskeletal 13		
	3	Q61781	K1C14_MOUSE	Keratin type I cytoskeletal 14		
	3	Q61414	K1C15_MOUSE	Keratin type I cytoskeletal 15		
	3	Q9Z2K1	K1C16_MOUSE	Keratin type I cytoskeletal 16		
	3	Q9QWL7	K1C17_MOUSE	Keratin type I cytoskeletal 17		
	3	P05784	K1C18_MOUSE	Keratin type I cytoskeletal 18		
	3	P19001	K1C19_MOUSE	Keratin type I cytoskeletal 19		
	3	Q3TTY5	K22E_MOUSE	Keratin type II cytoskeletal 2		
	3	P04104	K2C1_MOUSE	Keratin type II cytoskeletal 1		
	3	Q6IFZ6	K2C1B_MOUSE	Keratin type II cytoskeletal 1b		
	2	P07744	K2C4_MOUSE	Keratin type II cytoskeletal 4		
	3	Q922U2	K2C5_MOUSE	Keratin type II cytoskeletal 5		
	3	P50446	K2C6A_MOUSE	Keratin type II cytoskeletal 6A		
	3	Q9R0H5	K2C6G_MOUSE	Keratin type II cytoskeletal 6G		
	3	P11679	K2C8_MOUSE	Keratin type II cytoskeletal 8		
	3	Q99M73	KRT84_MOUSE	Keratin type II cuticular Hb4		
	3	P68369	TBA1_MOUSE	Tubulin alpha 1 chain		[46]
	3	P05214	TBA3_MOUSE	Tubulin alpha 3 alpha 7 chain		
	2	P68368	TBA4_MOUSE	Tubulin alpha 4 chain		
	2	Q9JJZ2	TBA8_MOUSE	Tubulin alpha 8 chain		
	3	P68372	TBB2C_MOUSE	Tubulin beta 2C chain	X	
	3	Q9D6F9	TBB4_MOUSE	Tubulin beta 4 chain	X	
	2	P99024	TBB5_MOUSE	Tubulin beta 5 chain		[39, 42, 44, 46]
	2	Q922F4	TBB6_MOUSE	Tubulin beta 6 chain	X	
Signaling	3	P62880	GBB2_MOUSE	Guanine nucleotide binding protein G I G S G T beta 2	X	
	3	Q9DAS9	GBG12_MOUSE	Guanine nucleotide binding protein G I G S G O gamma 12		
	3	Q99PT1	GDIR_MOUSE	Rho GDP dissociation inhibitor 1	X	
	2	P27601	GNA13_MOUSE	Guanine nucleotide binding protein alpha 13 subunit		
	2	P28667	MRP_MOUSE	MARCKS-related protein		
	3	P62835	RAP1A_MOUSE	Ras-related protein Rap 1A	X	
Membrane	2	Q8BSL7	ARF2_MOUSE	ADP ribosylation factor 2		
traffic	2	Q68FD5	CLH_MOUSE	Clathrin heavy chain	X	[42, 43, 46]
	2	P50396	GDIA_MOUSE	Rab GDP dissociation inhibitor alpha	X	
	2	Q61598	GDIB_MOUSE	Rab GDP dissociation inhibitor beta	X	[39, 45]
	3	Q9D1G1	RAB1B_MOUSE	Ras-related protein Rab 1B		
	3	P62991	UBIQ_MOUSE	Ubiquitin *Mus musculus* Mouse	X	[43, 46]
Chaperones	3	Q9CQV8	1433B_MOUSE	14 3 3 Protein beta alpha		[43]
	3	P62259	1433E_MOUSE	14 3 3 Protein epsilon	X	[43, 45]
	3	P68510	1433F_MOUSE	14 3 3 Protein eta		[39]
	3	P61982	1433G_MOUSE	14 3 3 Protein gamma	X	[39]

Table 1. Continued

	Detected	Accession	Entry	Description	Myelin proteome	References
	3	P68254	1433T_MOUSE	14 3 3 Protein theta		
	3	P63101	1433Z_MOUSE	14 3 3 Protein zeta delta	X	[39, 43, 46]
	3	P20029	GRP78_MOUSE	78 kDa Glucose regulated protein	X	
	2	Q61696	HS70A_MOUSE	Heat shock 70 kDa protein 1A		[45]
	2	P17879	HS70B_MOUSE	Heat shock 70 kDa protein 1B		
	3	P16627	HS70L_MOUSE	Heat shock 70 kDa protein 1L		
	3	P07901	HS90A_MOUSE	Heat shock protein HSP 90 alpha		[42, 44]
	3	P11499	HS90B_MOUSE	Heat shock protein HSP 90 beta		[39, 43, 44]
	3	P17156	HSP72_MOUSE	Heat shock-related 70 kDa protein 2		
	3	P63017	HSP7C_MOUSE	Heat shock cognate 71 kDa protein		[39, 42–46]
	3	P17742	PPIA_MOUSE	Peptidyl prolyl *cis trans* isomerase A	X	[43, 46]
Enzymes	3	O08553	DPYL2_MOUSE	Dihydropyrimidinase-related protein 2	X	
(oxidative	3	Q62188	DPYL3_MOUSE	Dihydropyrimidinase-related protein 3	X	
stress)	3	P19157	GSTP1_MOUSE	GST P 1	X	[45]
	3	P35700	PRDX1_MOUSE	Peroxiredoxin 1	X	[39]
	3	Q61171	PRDX2_MOUSE	Peroxiredoxin 2	X	
Enzymes	3	P05064	ALDOA_MOUSE	Fructose bisphosphate aldolase A	X	[42, 43]
(metabolism)	3	P00920	CAH2_MOUSE	Carbonic anhydrase 2 E	X	
	2	Q8BVI4	DHPR_MOUSE	Dihydropteridine reductase		
	3	P17182	ENOA_MOUSE	Alpha enolase	X	[42–45]
	3	P16858	G3P_MOUSE	Glyceraldehyde 3 phosphate dehydrogenase	X	[42–46]
	3	P13707	GPDA_MOUSE	Glycerol 3 phosphate dehydrogenase		
	3	Q04447	KCRB_MOUSE	Creatine kinase B type	X	
	3	P52480	KPYM_MOUSE	Pyruvate kinase isozyme M2	X	[42, 43, 46]
	3	P14152	MDHC_MOUSE	Malate dehydrogenase cytoplasmic	X	[45]
	3	P15532	NDKA_MOUSE	Nucleoside diphosphate kinase A	X	
	3	Q01768	NDKB_MOUSE	Nucleoside diphosphate kinase B	X	
	3	P09411	PGK1_MOUSE	Phosphoglycerate kinase 1	X	[43]
	2	P09041	PGK2_MOUSE	Phosphoglycerate kinase testis specific		
	3	Q8VDQ8	SIRT2_MOUSE	NAD dependent deacetylase sirtuin 2	X	
	3	Q93092	TALDO_MOUSE	Transaldolase		
	3	Q01853	TERA_MOUSE	Transitional ER ATPase		
	3	P40142	TKT_MOUSE	Transketolase	X	
	2	P17751	TPIS_MOUSE	Triosephosphate isomerase		[45]
	2	P61089	UBE2N_MOUSE	Ubiquitin conjugating enzyme E2		
Lipid	3	P08226	APOE_MOUSE	Apolipoprotein E		
metabolism	3	Q05816	FABPE_MOUSE	Fatty acid binding protein epidermal		
	3	Q9JL62	GLTP_MOUSE	Glycolipid transfer protein		
	3	P70296	PEBP1_MOUSE	Phosphatidylethanolamine binding protein 1	X	
Nucleus	3	P22752	H2A1_MOUSE	Histone H2A type 1		
	3	Q64523	H2A2C_MOUSE	Histone H2A type 2 C		
	3	P0C0S6	H2AZ_MOUSE	Histone H2A Z		
	3	P10853	H2B1F_MOUSE	Histone H2B type 1 F J L		[39]
	2	Q9D2U9	H2B3A_MOUSE	Histone H2B type 3 A		
	2	P68433	H31_MOUSE	Histone H3 1		
	3	P84228	H32_MOUSE	Histone H3 2		
	3	P62806	H4_MOUSE	Histone H4		[39, 43]
Ribosomes	3	P10126	EF1A1_MOUSE	Elongation factor 1 alpha 1	X	[39, 43]
	3	P62631	EF1A2_MOUSE	Elongation factor 1 alpha 2	X	
	3	P58252	EF2_MOUSE	Elongation factor 2	X	[45]

Classification was carried out according to Swiss-Prot entries and the literature. References for previous identification as exosomal proteins are given in the right column X, indicates identification in the myelin proteome [4-7].

neurons [48] (Fig. 6D, Table S1 in Supporting Information). As these studies partly used source material from other species, the identified proteins were mapped to the respective entries in the mouse Swiss-Prot database by a BLAST search. Only proteins with at least 90% sequence identity were considered to match. Among the 106 proteins identified in our study in at least two runs, 38 have been picked up by proteomic analyses of exosomes isolated from other cell types (Fig. 6D). A comparison with the recently published proteome of rat oligodendrocytes [49] revealed an overlap of 39 proteins (Table S1 in Supporting Information). Matching of our results with the myelin proteome [4–7] showed an intriguing overlap of 50 proteins, four of which are genuine myelin proteins. Apart from PLP and CNP, which were already identified by Western blotting, MBP and MOG were present in the exosomal fraction. The relative quantitative comparison of protein levels by MS signal response of the three most intense peptides [50] showed a strong enrichment of CNP and PLP with lower amounts MBP and MOG; thus, the relative abundance of myelin proteins in exosomes did not reflect the stoichiometry of the myelin membrane. Remarkably, exosomes and myelin share a similar configuration of enzymes, especially of those with a proposed function in oxidative stress. Moreover, exosomes are equipped with a plethora of chaperones of the heat shock protein family and the 14-3-3 protein family, which are adaptor proteins modulating the function of target proteins by recognition of phosphoserine or phosphothreonine motifs. Taken together, the results show a striking coenrichment of myelin components and enzymes associated with metabolism, signaling and cell stress in oligodendroglial exosomes.

3.4 Lipid analysis of oligodendroglial exosomes

Myelin has a specific lipid composition with high levels of glycosphingolipids and cholesterol. These lipids have been shown to participate in the formation of oligodendroglial lipid rafts [26]. Since lipid raft-mediated sorting is also involved in cargo selection during the formation of ILV [19], we asked if oligodendroglial exosomes are enriched in the classic myelin lipids, such as galactocerebroside and sulfatide. Primary cultured oligodendrocytes were cultured in the presence of [1-^{14}C]sodium acetate to allow its metabolic incorporation into fatty acids and to accumulate exosomes containing [1-^{14}C]-labeled lipids in the culture supernatant. Lipids extracted from exosomes, which had been purified by sucrose density gradient centrifugation, were analyzed by TLC followed by autoradiography and compared to total lipids from oligodendroglial membranes and purified CNS myelin membranes (Fig. 7). The unique myelin lipids galactocerebroside and sulfatide were indeed represented in the exosomal fraction. Cholesterol and phosphatidylcholine appear as most abundantly labeled lipid species in oligodendroglial exosomes, however this may relate to their synthesis and turnover rate and may not represent their actual relative enrichment.

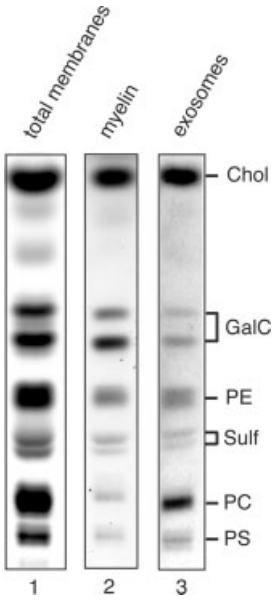

Figure 7. Lipid analysis of exosomes of oligodendroglial cells. Thin layer chromatograms of [1-^{14}C]acetate labeled lipids of total oligodendrocyte membranes (lane 1) or exosomes isolated by sucrose density gradient centrifugation (lane 3) as visualized by autoradiography, or lipids isolated from purified CNS myelin (lane 2). The mobility of reference lipids is indicated in the right. Myelin lipids and reference lipids were visualized by charring. Chol, cholesterol; GalC, galactocerebroside; Sulf, sulfatide; PE, phosphatidylethanolamine; PC, phosphatidylcholine; PS, phosphatidylserine.

4 Discussion

Myelination is the consequence of an intimate bidirectional cell–cell interaction between glia and neurons, resulting in long-term interdependence of the axon and the glial cell [1–3]. The mechanisms of myelin membrane biogenesis and the trafficking pathways of myelin components are only beginning to be unravelled [8, 51]. Exosomes are endosome-derived microvesicles that carry selected cargo and are released upon fusion of MVB with the plasma membrane into the extracellular space. Our study demonstrates that cultured oligodendrocytes secrete membrane vesicles with the typical characteristics of exosomes in a Ca^{2+}-dependent manner. They float on sucrose gradients at a density between 1.1 and 1.4 g/mL, have an average diameter of 30–80 nm, and contain typical exosomal markers such as Alix and Tsg101. Intriguingly, oligodendrolial exosomes contain a specific set of myelin components, such as PLP, CNP, MBP, and the typical myelin lipids. In addition, we find a striking accumulation of signaling proteins, chaperones and enzymes with a proposed function in the relief of cell stress.

4.1 Discrepancy in results between Western blotting and proteomic analysis

The methods we utilized to study the protein composition of oligodendroglial exosomes did not always yield identical results. For example, Na^+/K^+-ATPase was not detected in the exosomal fraction by Western blotting (and indeed was used as a control for contaminating plasma membrane fragments) but was identified as a component of exosomes by the proteomic analysis, as reported for B-cell- and microglia-derived exosomes before [44, 45]. In contrast, Alix and

Tsg101 were identified by Western blot analysis in the exosomal fractions, while they were not revealed by proteomic analysis. The sensitivity of the methods depends on both the potency of antibodies and the ionization efficiency of the peptides generated by trypsin digestion, respectively. It is thus possible that antibodies of high affinity specifically and directly detect low levels of distinct proteins, while they are below the detection limit of the proteome analysis and *vice versa*.

4.2 Signal-mediated release of exosomes

Our results demonstrate that oligodendroglial exosome release is enhanced by treatment of the cells with the Ca^{2+}-ionophore ionomycin, suggesting that MVB fusion and exosome secretion is controlled by free cytosolic Ca^{2+}-levels. This is in agreement with the general paradigm of secretion of lysosome-related organelles, which has been shown to depend on Ca^{2+} in cytotoxic T-cells, melanocytes, mast cells, and even fibroblasts, where this mode of membrane release contributes to plasma membrane repair after wounding [42, 43]. Ca^{2+}-dependent release of exosomes has initially been described in human leukemic cells [52, 53]. Interestingly, membrane depolarization in neurons leading to Ca^{2+} entry enhances the secretion of exosomes containing the GluR2/3 subunits of the AMPA-receptor suggesting that this mechanism may contribute to the fine-tuning of glutamate receptor levels present at synapses [48]. In oligodendrocytes, Ca^{2+}-signaling is mediated by neurotransmitters such as glutamate and ATP acting *via* ligand-gated and voltage-gated Ca^{2+}-channels [54]. Thus, cytoplasmic Ca^{2+}-levels in oligodendroglial cells and possibly also exosome release are likely to be coupled to neuronal activity. Future studies will address the influence of neurotransmitters on exosome secretion.

Recent work has demonstrated that neuronal signaling mediated by a soluble factor triggers the redistribution of PLP from late endosomal/lysosomal compartments to the oligodendroglial plasma membrane [11] and that Rho GTPase activity regulates the balance between endocytosis and exocytosis of PLP [55]. The present study shows that in response to Ca^{2+}-signaling, secretion of PLP in association with exosomes is enhanced. This mode of PLP trafficking is reminiscent of MHC class II trafficking in dendritic cells. In immature dendritic cells, the ILV of MVB serve as a storage site for MHC class II. Upon pathogen stimulation, MHC class II (loaded with antigenic peptides) redistribute to the plasma membrane, which is achieved by backfusion of the ILV with the limiting membrane and transfer of MHC class II to the plasma membrane *via* vesicular carriers [56]. Alternatively, dendritic cells secrete MHC carrying exosomes leading to stimulation of neighboring dendritic cells or T cells [57, 58]. In oligodendrocytes as in dendritic cells, late endosomal MVB thus constitute a dynamic membrane storage compartment that in response to external stimuli can reroute proteins to the plasma membrane or expose them to surrounding cells by secretion in association with exosomes.

4.3 Function of oligodendroglial exosomes

Exosome secretion has been described for several neural cell types, including neurons, astrocytes, and microglial cells [45, 48]. Furthermore, it has been shown that infectious prions and β-amyloid peptides are released in association with exosomes thus contributing by this means to pathogenesis in the nervous system [59, 60]. In all reports from neural tissue including ours, exosome release is limited to *in vitro* studies: however, validation *in situ* in a complex and tightly packed tissue such as the nervous system is difficult. Nonetheless, apart from the originally proposed role of exosomes in reticulocytes, where they are responsible for the eradication of obsolete membrane components, the release of exosomes carrying specific cargo encompasses an exciting concept of cell independent transport of messages between cells [16, 21]. Proof of this concept stems from the immune system where exosomes released from B-cells, dendritic cells, or tumor cells can elicit priming as well as tolerance reactions: exosomes thus harbor an enormous potential for the development of immunotherapies [23, 61]. Interestingly, a recent report describes genetic transfer between cells mediated by exosomes from mast cells containing mRNAs and microRNAs, that are functional upon exosome uptake by recipient cells [62].

What could be the physiological role of oligodendroglial exosome release? Secretion of a proteolytically cleaved C-terminal fragment of PLP has been detected earlier and an autotrophic role of PLP in oligodendroglial survival was proposed [63, 64]. However, we only detected unprocessed PLP and DM20 in exosomes and have not observed a cleavage product of PLP in our gel system. At first sight, the most evident function of oligodendroglial exosome release would seem to be the disposal of redundant myelin membrane produced by default by oligodendrocytes cultured in the absence of their neuronal partners. This concept is supported by the high degree of overlap between the oligodendroglial exosome and the myelin proteome. On the other hand, the similarities in composition between oligodendroglial exosomes and myelin may simply reflect that both membrane compartments are derived from the same cell type. A similar degree of overlap was found with the previously described proteome of exosomes from other cell types. Compared to the stoichiometry of the proteins in myelin, we find a striking enrichment of CNP in exosomes, while MBP, which should be almost as abundant as PLP, is under-represented. The specific sorting of PLP, CNP, and also MOG to exosomes is most likely facilitated by their association with lipid rafts [65, 66], which seem to act as sorting devices for exosomal membrane components [19]. Association of MBP with lipid rafts is developmentally regulated and depends on its phosphorylation [67] possibly explaining the low abundance of MBP in exosomes relative to PLP and CNP.

However, the secretion of overproduced myelin components *via* exosomes may play an important role in balancing myelin production *in vivo*. Overexpression of PLP or a block

in turnover of myelin glycosphingolipids leads to severe neurological disorders, characterized by dysmyelination and accumulation of these components in late endosomal/lysosomal compartments [39, 68]. It has been reported recently, that cells containing sulfatide-storing lysosomes can be induced to secrete sulfatide upon Ca^{2+} stimulation [69]. Release of membrane material from late endosomal compartments *via* exosomes may thus aid in relieving oligodendrocytes from the deleterious effects of overproduction or a lack of degradation of myelin components. Conceivably, the exosomes secreted by oligodendrocytes into the extracellular space could be removed by phagocytosis by microglial cells. Since microglia contribute to the immune system of the brain, it is important to mention the immune modulatory potential of exosomes, which could thus influence the course of myelin diseases. Indeed, PLP-overexpressing mice develop an immune response in the CNS, which contributes to myelin and axon degeneration in these animals [70]. The immune modulatory role of oligodendroglial exosomes may be of particular relevance for multiple sclerosis, where the interface between nervous system and immune system plays a pivotal role. MBP and MOG are major autoantigens in multiple sclerosis and myelin disease models and an immune response to specific regions of PLP is often exhibited by patients in early phases of the disease [71, 72]. Exosomes exposed to phagocytic microglia/monocytes may thus modulate activation of these cells or may even signal to T- and B-cells which have invaded the nervous system by passing the blood brain barrier and are involved in the pathogenesis.

Another exiting potential function of oligodendroglial exosomes is their possible role in transcellular signaling between glia cell and axon. With myelination, axon and oligodendroctye develop a close interdependence and myelin loss leads to secondary axonal degeneration [2, 73]. A similar axonal degeneration involving swellings and defects in axonal transport is observed upon genetic ablation of either PLP or CNP, although the myelin sheath is morphologically intact [74, 75]. Thus, axons receive vital trophic support from oligodendroglial cells, the nature of which is largely unelucidated. Intriguingly, both PLP and CNP are major components of oligodendroglial exosomes together with a plethora of chaperones and enzymes involved in the management of oxidative stress. It is thus tempting to speculate that oligodendroglial exosomes might carry essential trophic factors towards the axon. Indeed, transfer of heat shock proteins from glia to axons has been reported [76]. Moreover, intracellularly injected horseradish peroxidase is transferred from myelinating oligodendrocytes to axons in the paranodal region in the rat optic nerve [77], and in squid it is well documented, that transport of molecules from the ensheathing glial cell to the giant axon involves membrane-bound vesicles [78].

In conclusion, the Ca^{2+}-dependent secretion of exosomes by oligodendroglial cells encompasses intriguing potential functions. In crosstalk with neurons, oligodendrocytes may secrete exosomes to balance the cellular levels of membrane components involved in myelin synthesis and turnover. Additionally, exosomes may deliver trophic molecules to the axon. It is important to elucidate the physiological role of exosomes during development and in diseases involving myelin.

We thank Ulrike Stapf, Lilja Niedens, and Jasmin Forsch for expert technical assistance. This study was supported by grants from the Deutsche Forschungsgemeinschaft (Sonderforschungsbereich 490, E6, Z3) to S. T. and H. S., Hochschulbauförderungsgesetz Programme (HBFG-122-605) to H. S., the EU SP6 "Signalling and Traffic" to J. T., and the European Leukodystrophy Association to E. -M. K. -A..

5 References

[1] Salzer, J. L., Polarized domains of myelinated axons. *Neuron* 2003, *40*, 297–318.

[2] Popko, B., Myelin: Not just a conduit for conduction. *Nat. Genet.* 2003, *33*, 327–328.

[3] Sherman, D. L., Brophy, P. J., Mechanisms of axon ensheathment and myelin growth. *Nat. Rev. Neurosci.* 2005, *6*, 683–690.

[4] Taylor, C. M., Marta, C. B., Claycomb, R. J., Han, D. K. *et al.*, Proteomic mapping provides powerful insights into functional myelin biology. *Proc. Natl. Acad. Sci. USA* 2004, *101*, 4643–4648.

[5] Vanrobaeys, F., Van Coster, R., Dhondt, G., Devreese, B., Van Beeumen, J., Profiling of myelin proteins by 2D-gel electrophoresis and multidimensional liquid chromatography coupled to MALDI TOF-TOF mass spectrometry. *J. Proteome Res.* 2005, *4*, 2283–2293.

[6] Huang, J. K., Phillips, G. R., Roth, A. D., Pedraza, L. *et al.*, Glial membranes at the node of Ranvier prevent neurite outgrowth. *Science* 2005, *310*, 1813–1817.

[7] Roth, A. D., Ivanova, A., Colman, D. R., New observations on the compact myelin proteome. *Neuron Glia Biol.* 2006, *2*, 15–21.

[8] Kramer, E. M., Schardt, A., Nave, K. A., Membrane traffic in myelinating oligodendrocytes. *Microsci. Res. Tech.* 2001, *52*, 656–671.

[9] Larocca, J. N., Rodriguez-Gabin, A. G., Myelin biogenesis: Vesicle transport in oligodendrocytes. *Neurochem. Res.* 2002, *27*, 1313–1329.

[10] Simons, M., Trajkovic, K., Neuron-glia communication in the control of oligodendrocyte function and myelin biogenesis. *J. Cell. Sci.* 2006, *119*, 4381–4389.

[11] Trajkovic, K., Dhaunchak, A. S., Goncalves, J. T., Wenzel, D. *et al.*, Neuron to glia signaling triggers myelin membrane exocytosis from endosomal storage sites. *J. Cell Biol.* 2006, *172*, 937–948.

[12] van der Goot, F. G., Gruenberg, J., Intra-endosomal membrane traffic. *Trends Cell Biol.* 2006, *16*, 514–521.

[13] Thery, C., Zitvogel, L., Amigorena, S., Exosomes: Composition, biogenesis and function. *Nat. Rev. Immunol.* 2002, *2*, 569–579.

[14] Keller, S., Sanderson, M. P., Stoeck, A., Altevogt, P., Exosomes: From biogenesis and secretion to biological function. *Immunol. Lett.* 2006, *107*, 102–108.

[15] van Niel, G., Porto-Carreiro, I., Simoes, S., Raposo, G., Exosomes: A common pathway for a specialized function. *J. Biochem. (Tokyo)* 2006, *140*, 13–21.

[16] Fevrier, B., Raposo, G., Exosomes: Endosomal-derived vesicles shipping extracellular messages. *Curr. Opin. Cell Biol.* 2004, *16*, 415–421.

[17] Raiborg, C., Rusten, T. E., Stenmark, H., Protein sorting into multivesicular endosomes. *Curr. Opin. Cell Biol.* 2003, *15*, 446–455.

[18] Slagsvold, T., Pattni, K., Malerod, L., Stenmark, H., Endosomal and non-endosomal functions of ESCRT proteins. *Trends Cell Biol.* 2006, *16*, 317–326.

[19] de Gassart, A., Geminard, C., Fevrier, B., Raposo, G., Vidal, M., Lipid raft-associated protein sorting in exosomes. *Blood* 2003, *102*, 4336–4344.

[20] Hemler, M. E., Tetraspanin proteins mediate cellular penetration, invasion, and fusion events and define a novel type of membrane microdomain. *Ann. Rev. Cell Dev. Biol.* 2003, *19*, 397–422.

[21] Johnstone, R. M., Exosomes biological significance: A concise review. *Blood Cells Mol. Dis.* 2006, *36*, 315–321.

[22] Pan, B. T., Teng, K., Wu, C., Adam, M., Johnstone, R. M., Electron microscopic evidence for externalization of the transferrin receptor in vesicular form in sheep reticulocytes. *J. Cell Biol.* 1985, *101*, 942–948.

[23] Li, X. B., Zhang, Z. R., Schluesener, H. J., Xu, S. Q., Role of exosomes in immune regulation. *J. Cell. Mol. Med.* 2006, *10*, 364–375.

[24] Greco, V., Hannus, M., Eaton, S., Argosomes: A potential vehicle for the spread of morphogens through epithelia. *Cell* 2001, *106*, 633–645.

[25] Liegeois, S., Benedetto, A., Garnier, J. M., Schwab, Y., Labouesse, M., The V0-ATPase mediates apical secretion of exosomes containing Hedgehog-related proteins in Caenorhabditis elegans. *J. Cell Biol.* 2006, *173*, 949–961.

[26] Kramer, E. M., Koch, T., Niehaus, A., Trotter, J., Oligodendrocytes direct glycosyl phosphatidylinositol-anchored proteins to the myelin sheath in glycosphingolipid-rich complexes. *J. Biol. Chem.* 1997, *272*, 8937–8945.

[27] Trotter, J., Bitter-Suermann, D., Schachner, M., Differentiation-regulated loss of the polysialylated embryonic form and expression of the different polypeptides of the neural cell adhesion molecule by cultured oligodendrocytes and myelin. *J. Neurosci. Res.* 1989, *22*, 369–383.

[28] Jung, M., Kramer, E., Grzenkowski, M., Tang, K. *et al.*, Lines of murine oligodendroglial precursor cells immortalized by an activated neu tyrosine kinase show distinct degrees of interaction with axons *in vitro* and *in vivo*. *Eur. J. Neurosci.* 1995, *7*, 1245–1265.

[29] Norton, W. T., Poduslo, S. E., Myelination in rat brain: Method of myelin isolation. *J. Neurochem.* 1973, *21*, 749–757.

[30] Laemmli, U. K., Cleavage of structural proteins during the assembly of the head of bacteriophage T4. *Nature* 1970, *227*, 680–685.

[31] Liou, W., Geuze, H. J., Slot, J. W., Improving structural integrity of cryosections for immunogold labeling. *Histochem. Cell Biol.* 1996, *106*, 41–58.

[32] Skilling, J., Denny, R., Richardson, K., Young, P. *et al.*, Probseq—a fragmentation model for interpretation of electrospray tandem mass spectrometry data. *Comp. Funct. Genomics* 2004, *5*, 61–68.

[33] Silva, J. C., Denny, R., Dorschel, C. A., Gorenstein, M. *et al.*, Quantitative proteomic analysis by accurate mass retention time pairs. *Anal. Chem.* 2005, *77*, 2187–2200.

[34] Silva, J. C., Denny, R., Dorschel, C., Gorenstein, M. V. *et al.*, Simultaneous qualitative and quantitative analysis of the *Escherichia coli* proteome: A sweet tale. *Mol. Cell. Proteomics* 2006, *5*, 589–607.

[35] Vissers, J. P., Langridge, J. I., Aerts, J. M., Analysis and quantification of diagnostic serum markers and protein signatures for Gaucher disease. *Mol. Cell. Proteomics* 2007, *6*, 755–766.

[36] Li, G.-Z., Golick, D., Gorenstein, M. V., Silvia, J. C., et al.,A novel ion accounting algorithm for protein database searches. *Poster W079 Presented at the Human Proteome Organisation (HUPO) 5th Annual World Congress*, 2006, October 28–November 1, Long Beach, CA.

[37] Horton, P., Park, K. J., Obayashi, T., Fujita, N. *et al.*, WoLF PSORT: Protein localization predictor. *Nucleic Acids Res.* 2007, *35*, W585–W587.

[38] Bligh, E. G., Dyer, W. J., A rapid method of total lipid extraction and purification. *Can. J. Biochem. Physiol.* 1959, *37*, 911–917.

[39] Simons, M., Kramer, E. M., Macchi, P., Rathke-Hartlieb, S. *et al.*, Overexpression of the myelin proteolipid protein leads to accumulation of cholesterol and proteolipid protein in endosomes/lysosomes: Implications for Pelizaeus-Merzbacher disease. *J. Cell Biol.* 2002, *157*, 327–336.

[40] Geminard, C., De Gassart, A., Blanc, L., Vidal, M., Degradation of AP2 during reticulocyte maturation enhances binding of hsc70 and Alix to a common site on TFR for sorting into exosomes. *Traffic* 2004, *5*, 181–193.

[41] Thery, C., Boussac, M., Veron, P., Ricciardi-Castagnoli, P. *et al.*, Proteomic analysis of dendritic cell-derived exosomes: A secreted subcellular compartment distinct from apoptotic vesicles. *J. Immunol.* 2001, *166*, 7309–7318.

[42] Stinchcombe, J., Bossi, G., Griffiths, G. M., Linking albinism and immunity: The secrets of secretory lysosomes. *Science* 2004, *305*, 55–59.

[43] Reddy, A., Caler, E. V., Andrews, N. W., Plasma membrane repair is mediated by Ca(2+)-regulated exocytosis of lysosomes. *Cell* 2001, *106*, 157–169.

[44] Wubbolts, R., Leckie, R. S., Veenhuizen, P. T., Schwarzmann, G. *et al.*, Proteomic and biochemical analyses of human B cell-derived exosomes. Potential implications for their function and multivesicular body formation. *J. Biol. Chem.* 2003, *278*, 10963–10972.

[45] Potolicchio, I., Carven, G. J., Xu, X., Stipp, C. *et al.*, Proteomic analysis of microglia-derived exosomes: Metabolic role of the aminopeptidase CD13 in neuropeptide catabolism. *J. Immunol.* 2005, *175*, 2237–2243.

[46] Hegmans, J. P., Bard, M. P., Hemmes, A., Luider, T. M. *et al.*, Proteomic analysis of exosomes secreted by human mesothelioma cells. *Am. J. Pathol.* 2004, *164*, 1807–1815.

[47] Mears, R., Craven, R. A., Hanrahan, S., Totty, N. *et al.*, Proteomic analysis of melanoma-derived exosomes by two-dimensional polyacrylamide gel electrophoresis and mass spectrometry. *Proteomics* 2004, *4*, 4019–4031.

[48] Faure, J., Lachenal, G., Court, M., Hirrlinger, J. *et al.*, Exosomes are released by cultured cortical neurones. *Mol. Cell. Neurosci.* 2006, *31*, 642–648.

[49] Dumont, D., Noben, J. P., Moreels, M., Vanderlocht, J. *et al.*, Characterization of mature rat oligodendrocytes: A proteomic approach. *J. Neurochem.* 2007, *102*, 562–576.

[50] Silva, J. C., Gorenstein, M. V., Li, G. Z., Vissers, J. P., Geromanos, S. J., Absolute quantification of proteins by LCMSE: A virtue of parallel MS acquisition. *Mol. Cell. Proteomics* 2006, *5*, 144–156.

[51] Anitei, M., Pfeiffer, S. E., Myelin biogenesis: Sorting out protein trafficking. *Curr. Biol.* 2006, *16*, R418–R421.

[52] Savina, A., Furlan, M., Vidal, M., Colombo, M. I., Exosome release is regulated by a calcium-dependent mechanism in K562 cells. *J. Biol. Chem.* 2003, *278*, 20083–20090.

[53] Savina, A., Fader, C. M., Damiani, M. T., Colombo, M. I., Rab11 promotes docking and fusion of multivesicular bodies in a calcium-dependent manner. *Traffic* 2005, *6*, 131–143.

[54] Butt, A. M., Neurotransmitter-mediated calcium signalling in oligodendrocyte physiology and pathology. *Glia* 2006, *54*, 666–675.

[55] Kippert, A., Trajkovic, K., Rajendran, L., Ries, J., Simons, M., Rho regulates membrane transport in the endocytic pathway to control plasma membrane specialization in oligodendroglial cells. *J. Neurosci.* 2007, *27*, 3560–3570.

[56] Kleijmeer, M., Ramm, G., Schuurhuis, D., Griffith, J. *et al.*, Reorganization of multivesicular bodies regulates MHC class II antigen presentation by dendritic cells. *J. Cell Biol.* 2001, *155*, 53–63.

[57] Thery, C., Duban, L., Segura, E., Veron, P. *et al.*, Indirect activation of naive CD4+ T cells by dendritic cell-derived exosomes. *Nat. Immunol.* 2002, *3*, 1156–1162.

[58] Stoorvogel, W., Kleijmeer, M. J., Geuze, H. J., Raposo, G., The biogenesis and functions of exosomes. *Traffic* 2002, *3*, 321–330.

[59] Fevrier, B., Vilette, D., Archer, F., Loew, D. *et al.*, Cells release prions in association with exosomes. *Proc. Natl. Acad. Sci. USA* 2004, *101*, 9683–9688.

[60] Rajendran, L., Honsho, M., Zahn, T. R., Keller, P. *et al.*, Alzheimer's disease beta-amyloid peptides are released in association with exosomes. *Proc. Natl. Acad. Sci. USA* 2006, *103*, 11172–11177.

[61] Mignot, G., Roux, S., Thery, C., Segura, E., Zitvogel, L., Prospects for exosomes in immunotherapy of cancer. *J. Cell. Mol. Med.* 2006, *10*, 376–388.

[62] Valadi, H., Ekstrom, K., Bossios, A., Sjostrand, M. *et al.*, Exosome-mediated transfer of mRNAs and microRNAs is a novel mechanism of genetic exchange between cells. *Nat. Cell Biol.* 2007, *9*, 654–659.

[63] Yamada, M., Ivanova, A., Yamaguchi, Y., Lees, M. B., Ikenaka, K., Proteolipid protein gene product can be secreted and exhibit biological activity during early development. *J. Neurosci.* 1999, *19*, 2143–2151.

[64] Knapp, P. E., Bartlett, W. P., Williams, L. A., Yamada, M. *et al.*, Programmed cell death without DNA fragmentation in the jimpy mouse: Secreted factors can enhance survival. *Cell Death Differ.* 1999, *6*, 136–145.

[65] Simons, M., Kramer, E. M., Thiele, C., Stoffel, W., Trotter, J., Assembly of myelin by association of proteolipid protein with cholesterol- and galactosylceramide-rich membrane domains. *J. Cell Biol.* 2000, *151*, 143–154.

[66] Kim, T., Pfeiffer, S. E., Myelin glycosphingolipid/cholesterol-enriched microdomains selectively sequester the non-compact myelin proteins CNP and MOG. *J. Neurocytol.* 1999, *28*, 281–293.

[67] DeBruin, L. S., Haines, J. D., Wellhauser, L. A., Radeva, G. *et al.*, Developmental partitioning of myelin basic protein into membrane microdomains. *J. Neurosci. Res.* 2005, *80*, 211–225.

[68] Gieselmann, V., Franken, S., Klein, D., Mansson, J. E. *et al.*, Metachromatic leukodystrophy: Consequences of sulphatide accumulation. *Acta Paediatr. Suppl.* 2003, *92*, 74–79; discussion 45.

[69] Klein, D., Bussow, H., Fewou, S. N., Gieselmann, V., Exocytosis of storage material in a lysosomal disorder. *Biochem. Biophys. Res. Commun.* 2005, *327*, 663–667.

[70] Ip, C. W., Kroner, A., Bendszus, M., Leder, C. *et al.*, Immune cells contribute to myelin degeneration and axonopathic changes in mice overexpressing proteolipid protein in oligodendrocytes. *J. Neurosci.* 2006, *26*, 8206–8216.

[71] Hauser, S. L., Oksenberg, J. R., The neurobiology of multiple sclerosis: Genes, inflammation, and neurodegeneration. *Neuron* 2006, *52*, 61–76.

[72] Tuohy, V. K., Yu, M., Weinstock-Guttman, B., Kinkel, R. P., Diversity and plasticity of self recognition during the development of multiple sclerosis. *J. Clin. Invest.* 1997, *99*, 1682–1690.

[73] Trapp, B. D., Andrews, S. B., Cootauco, C., Quarles, R., The myelin-associated glycoprotein is enriched in multivesicular bodies and periaxonal membranes of actively myelinating oligodendrocytes. *J. Cell Biol.* 1989, *109*, 2417–2426.

[74] Griffiths, I., Klugmann, M., Anderson, T., Yool, D. *et al.*, Axonal swellings and degeneration in mice lacking the major proteolipid of myelin. *Science* 1998, *280*, 1610–1613.

[75] Lappe-Siefke, C., Goebbels, S., Gravel, M., Nicksch, E. *et al.*, Disruption of Cnp1 uncouples oligodendroglial functions in axonal support and myelination. *Nat. Genet.* 2003, *33*, 366–374.

[76] Tytell, M., Release of heat shock proteins (Hsps) and the effects of extracellular Hsps on neural cells and tissues. *Int. J. Hyperthermia* 2005, *21*, 445–455.

[77] Duncan, A., Ibrahim, M., Berry, M., Butt, A. M., Transfer of horseradish peroxidase from oligodendrocyte to axon in the myelinating neonatal rat optic nerve: Artefact or transcellular exchange? *Glia* 1996, *17*, 349–355.

[78] Buchheit, T. E., Tytell, M., Transfer of molecules from glia to axon in the squid may be mediated by glial vesicles. *J. Neurobiol.* 1992, *23*, 217–230.

